Sensing and Bio-Sensing Research 17 (2018) 1–6

Contents lists available at ScienceDirect

Sensing and Bio-Sensing Research

journal homepage: www.elsevier.com/locate/sbsr

Conductive composites for oligonucleotide detection☆

David C. Ferrier[a], Michael P. Shaver[b], Philip J.W. Hands[a,*]

[a] Institute for Integrated Micro and Nano Systems, School of Engineering, University of Edinburgh, Edinburgh EH9 3JL, UK
[b] School of Chemistry, David Brewster Road, University of Edinburgh, EH9 3FJ, UK

ARTICLE INFO

Keywords:
Oligonucleotide sensor
DNA sensor
Bio-responsive
Nanocomposite
Hydrogel
Smart material

ABSTRACT

A new method for oligonucleotide detection is presented based on oligonucleotide cross-linked polymer composites. Conductive carbon nanoparticles are incorporated into a DNA-functionalised polymer, containing partially complementary oligonucleotide cross-linkers, which is polymerised *in situ* upon interdigitated electrodes. In the presence of an aqueous solution of a specific analyte oligonucleotide sequence, the cross-linkers are cleaved, leading to increased swelling. As the polymer swells the relative density of the conductive particles decreases, leading to an easily measurable decrease in electrical conductivity. We demonstrate that such are capable of discriminating between analyte and control solutions, with single-base specificity, in under 3 min. The lower detection limit of these composites is of the order of 10 nM. The swelling characteristics of these composites is confirmed by optical imaging and the effects of varying temperature upon such composites are also reported.

1. Introduction

Conductive composites, wherein conductive particles are mixed into a non-conductive polymer matrix, have long been applied to chemical sensing in fields such as electronic noses and tongues [1–8]. In such applications, the conductive component is added to the non-conductive polymer in sufficient quantities to form conductive pathways throughout the composite, referred to as a percolating state [8]. The presence of certain molecules, often volatile organic compounds (VOCs), cause the polymers to swell, resulting in the breaking of conductive pathways and a decrease of the electrical conductivity. Generally such chemical sensors are ambiguous in their response, but arrays of these, with each element prepared with different polymers, coupled with pattern recognition techniques can provide specific discrimination. To date there have been few successful applications of such swelling, percolating composites to biosensing [9]. This may be due to the lack of specificity of an adsorptive swelling mechanism coupled to the often low concentration of biological molecules of interest.

We hypothesized that designing the system to inherently amplify the swelling from a biomolecule could permit percolating composite biosensing. Stokke et al. have developed DNA-functionalised polymers that demonstrate selective swelling in the presence of specific oligonucleotide sequences [10–12]. Such polymers contain both conventional chemical cross-linkers and oligonucleotide cross-linkers, comprised of two, partially complementary, oligonucleotide sequences (Fig. 1). In the presence of analyte oligonucleotides (to which the 'sensor' strand is perfectly complementary) the 'blocker' strand will be displaced, causing the cross-link to break. This selective cleavage of cross-links leads to changes in the swelling behaviour of the polymer, resulting in increased swelling.

This paper outlines preliminary efforts to develop conductive composites based on such DNA-functionalised polymers, in the hope of providing a simple, rapid and low-cost means of transduction for multiplexed oligonucleotide sensing applications ranging from point-of-care diagnostics [13–15] to forensic science [16,17]. To date, only optical transduction methods have been applied to these polymers [10–12], which, whilst effective, presents potential cost, portability and multiplexing challenges.

We report the development of an Oligonucleotide Cross-linked Polymer Composite (OCPC) that demonstrates highly selective swelling in the presence of analyte oligonucleotides and whose resistance decreases with swelling. Analyte solutions can be clearly differentiated from control solutions, with single-base specificity, in under 3 min *via* differences in the rate of transition between percolating and non-percolating states.

2. Materials & methods

2.1. Materials

Acrylamide (AAM), methylene-bisacrylamide (MBA), hydroxycyclohexyl phenyl ketone (HPK), ethylene glycol, trimethoxysilyl propyl methacrylate (TPM), hydrochloric acid (HCl), phosphate buffer

☆ Selected paper from the 5th International Conference on Bio-Sensing Technology, 7-10 May 2017, Riva del Garda, Italy.

* Corresponding author.
E-mail address: philip.hands@ed.ac.uk (P.J.W. Hands).

https://doi.org/10.1016/j.sbsr.2017.11.007
Received 29 August 2017; Accepted 22 November 2017

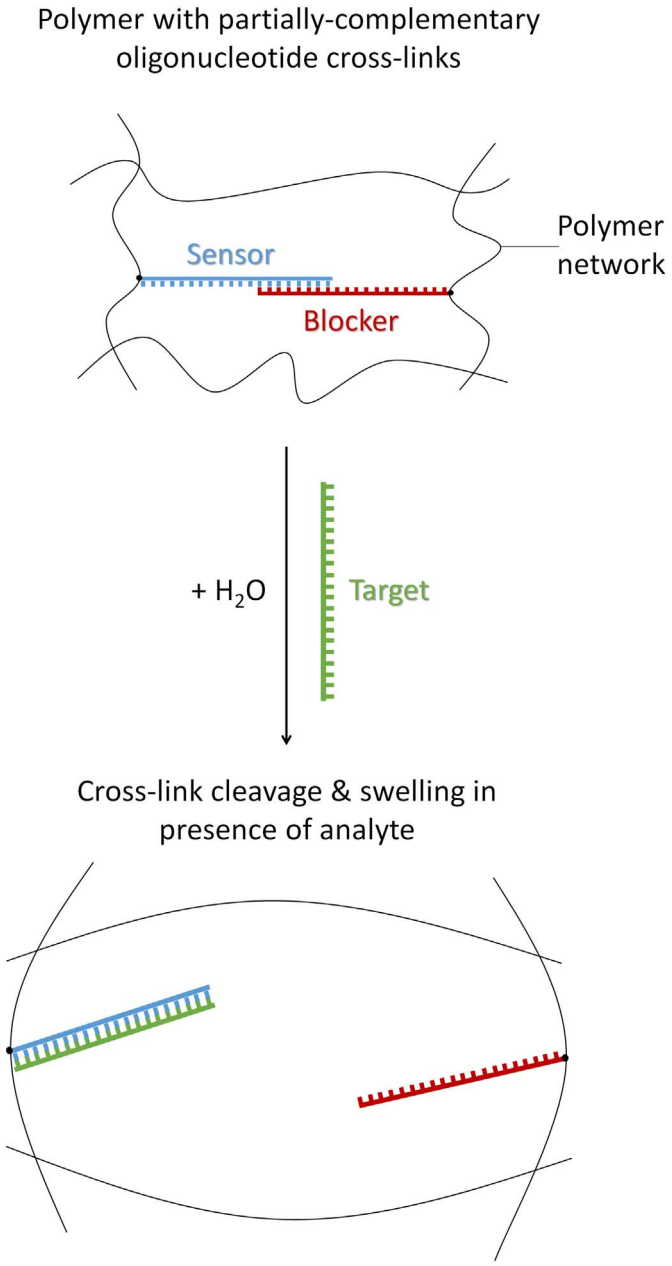

Fig. 1. The sensing mechanism of oligonucleotide-functionalised polymers. (Adapted from Tierney and Stokke [10]).

(1 M, pH 7.4) and carbon nanopowder (< 50 nm) were purchased from Sigma-Aldrich and used as received. Aqueous stock solutions of AAM and MBA were prepared (150 mM NaCl, 1 mM phosphate buffer) as was a stock solution of the HPK photo-initiator in ethylene glycol.

The oligonucleotide sequences were purchased from Integrated DNA Technologies. They include sensor (S) and blocker (B) sequences (Fig. 1), a fully complementary analyte sequence (A_0), a five-mismatch sequence (A_5), a single-mismatch sequence (A_1) and a random control sequence (R). The S and B sequences were supplied functionalised with an Acrydite modifier and have a 12-base complementary region at their respective 3′ ends (Fig. 2). The S and B sequences were mixed together in equal concentrations, before being extracted from solution using a standard ethanol precipitation. All other oligonucleotide sequences were suspended at various concentrations (ranging from 1 nM to 10 μM) in aqueous buffer solutions (150 mM NaCl, 1 mM phosphate buffer).

2.2. Composite synthesis

The AAM, MBA and HPK stocks were mixed together in appropriate volumes to form a 10 wt% AAM gelator solution (0.6 mol% w.r.t. monomer MBA, 0.125 mol% w.r.t. monomer HPK). Carbon nanopowder was added to this solution at concentrations ranging between 0 and 20 mg/mL and dispersed *via* manual agitation. This mixture was added to the dried S/B oligonucleotides and the oligonucleotides allowed to fully dissolve, producing an oligonucleotide concentration of 0.4 mol% w.r.t. monomer. Full details of the composite synthesis can be found in the Supplementary information.

After mixing, droplets of this pre-composite solution were pipetted onto substrates and polymerised by exposure to UV radiation for 60 s using an arc lamp (Dymax Bluewave 75, 280–450 nm, > 19 W/cm^2) to form an OCPC.

2.3. Electrode fabrication

The electrode devices consisted of platinum Interdigitated Electrodes (IDEs) fabricated on a silicon/silicon dioxide substrate. The IDE arrays covered an area of 1.5 × 1.5 mm and contained 30 digits, each 10 μm wide and separated by 40 μm. They were fabricated using standard photolithography procedures. The substrates were silanised using a procedure adapted from Tierney et al. [18], so as to improve the adhesion of the composites. The devices were immersed in a 0.01 M HCl solution for approximately 10 min before immersing them in TPM in acetone (0.02 M) for 1 h. Further details on the electrode fabrication and silanisation can be found in the Supplementary information.

2.4. Optical measurements

Optical volume measurements enabled the simple determination of OCPC swelling responses before testing their conductivity changes as a result of that swelling. OCPC droplets were prepared as described in Section 2.2 and polymerised *in situ* on the electrode devices described in Section 2.3. These samples were partially dried out under refrigeration (3 ± 1)°C before being immersed in various oligonucleotide solutions (A_0, A_1, A_5 and R) at concentrations ranging between 1 nM and 10 μM. The samples were either imaged as they swell in these solutions (as shown in Fig. 3) or swollen to equilibrium at temperatures ranging from 3 to 37 °C, removed from solution, patted dry and imaged in air (Fig. 3). The carbon concentrations were either 0 or 10 mg/mL and for these experiments carbon was added solely as a contrast agent. Further details on the optical measurements can be found in the Supplementary information.

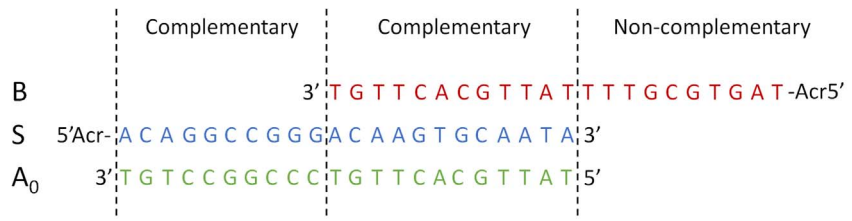

Fig. 2. The sequences and respective complementarity of the S, B and A_0 oligonucleotide sequences. 'Acr' denotes the acrydite modifier. The vertical dashed lines delineate the respective regions of complementarity.

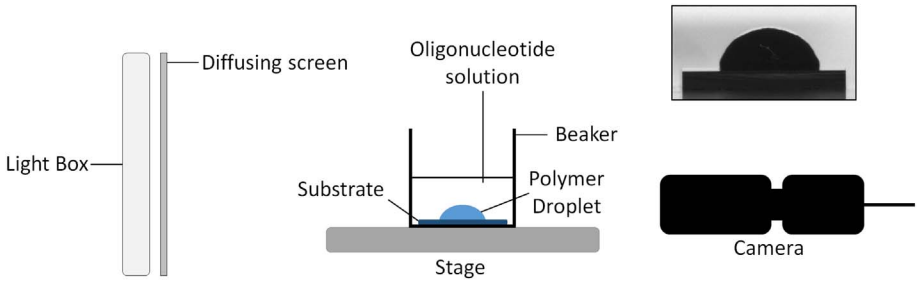

Fig. 3. Optical measurement set-up – The samples were placed in solution on the stage and imaged using a Sony XCD-X710 Firewire camera in conjunction with IC Capture image acquisition software. Samples can also be removed from the solution, patted dry and imaged independently. The droplet volumes are then determined using a custom MatLab algorithm. The measurement set-up is housed in a temperature controlled environment, held at (20 ± 1)°C. Inset top right – example image of an OCPC droplet on a silicon substrate.

2.5. Electrical measurements

2 μL droplets of OCPC (20 mg/mL carbon) were prepared as described previously. These samples were allowed to partially dry out under refrigeration for 24 h, before being immersed in A_0 or R solutions of varying concentration and their electrical resistance measured as they swell using a Keithley 2000 digital multimeter and a 2-terminal resistance measurement. The solutions were held at 23 °C using a water bath.

3. Results & discussion

3.1. Optical measurements

It is believed that a measurement of the electrical resistance of an OCPC can provide a simple, low-cost and rapid means of detecting a given analyte oligonucleotide sequence. In order to confirm that any changes to the electrical properties are a result of the selective swelling of the composite, it is necessary to determine the swelling characteristics of OCPCs. This swelling behaviour was measured by imaging immobilised OCPC droplets, in different oligonucleotide solutions and varying temperatures, and calculating their volume by image analysis.

Fig. 4 A shows the fractional volume change, δ_v, for OCPC droplets in either 10 μM A_0 or R solutions, defined as:

$$\delta_v = \frac{V - V_i}{V_i} \tag{1}$$

where V is the measured volume of the swelling droplet and V_i is the initial droplet volume, prior to polymerisation. Given that, as described in Section 2.4, the OCPC samples are partially dried before swelling, their volume at $t = 0$ will be below V_i. Hence, at early times during swelling, δ_v will be negative. δ_v is defined relative to V_i as this represents the most stable reference point with the lowest experimental error. Samples in A_0 solutions swell to significantly larger volumes (with δ_v values of approximately 0.6 as opposed to 0.2 for R solutions) as a result of the selective cleavage of oligonucleotide cross-linkers. Given the differences in experimental techniques it is difficult to make a direct comparison with the swelling magnitudes reported by Stokke et al. [10–12]. However, assuming spherical geometry it is possible to determine that approximate δ_v values for the maximum swelling they report in fully complementary analyte solutions are of the same order of magnitude as the values reported here.

The majority of the swelling appears complete within 1 h but the differences between the A_0 and R samples are apparent within 10 min. Fig. 4 B shows the same data for A_0 solutions of varying concentration. For concentrations ranging from 10 μM to 100 nM the OCPCs show highly similar swelling behaviour, within the bounds of experimental uncertainty. The swelling behaviour begins to diverge at concentrations of the order of 10 nM, at which the initial rate of swelling is the same for higher concentrations, but slows after approximately 5 min and tends towards a lower equilibrium volume, similar to that of samples in R solutions. At concentrations of 1 nM both the initial rate of swelling and equilibrium volume are similar to OCPC samples in R solutions.

In the work of Stokke et al. the rate of swelling demonstrated a dependency on the analyte concentration [10,11]. Such behaviour is not evident here. This is most likely a result of the fact that the hydrogel droplets in these experiments are significantly larger than those created by Stokke et al. As such the swelling time of the gel network has increased to the point where it is a limiting factor. The rate of swelling only begins to change where there is a difference in the equilibrium volume of the OCPCs, at concentrations of 10 nM and below. This corresponds to existing models of hydrogel swelling, such as presented by Tanaka et al., which show that the rate of swelling is dependent only upon the final swelling volume and the diffusion coefficient [19]. The limits at which selective swelling is observed to occur in Fig. 4 correspond to what has been reported by Stokke et al. [10] (despite employing a far less sensitive measurement technique). It is likely that, if the OCPC volume were to be sufficiently reduced, a dependency of the rate of swelling upon analyte concentration would begin to manifest as the swelling became dependent upon the rate of cross-link cleavage.

Fig. 5 shows δ_v for OCPCs after 1 h of immersion in oligonucleotide solutions with varying degrees of complementarity to the analyte sequence, A_0. The selective swelling response between solutions containing analyte and random oligonucleotides is clearly evident. Samples immersed in solutions in which the oligonucleotides differ by only 5 (A_5) or 1 (A_1) bases display swelling comparable to those immersed in random solutions, indicating little or no cross-link cleavage, beyond that due to thermal effects. It is clear from Fig. 5 that OCPCs display high selectivity, with their differential swelling characteristics being evident even between samples differing by a single nucleotide.

Fig. 6 shows δ_v as a function of temperature for OCPCs in both 10 μM A_0 and R solutions. In both cases the experimental data is shown alongside a least-squares fit to a sigmoidal function, also known as the four parametric logistic model [20–22]. There is considerable variation, with δ_v ranging from approximately 0.5 to 1.2 in A_0 solutions and − 0.1 and 1.0 in R solutions. This variation is due to the thermal dehybridisation of the oligonucleotide cross-linkers. At low temperatures (< 15 °C) there is little thermal dehybridisation and δ_v remains low. As the temperature increases δ_v begins to increase rapidly as the degree of thermal dehybridisation increases, until at high temperatures (> 40 °C) almost all the oligonucleotide cross-linkers are thermally de-hybridised and δ_v reaches a plateau, resulting in the characteristic sigmoid curves seen in Fig. 6. Whilst the immersion in solution takes place at varying temperature, the fact that the volume measurement takes place at room temperature and that the small OCPC samples will rapidly return to ambient temperature mean that any swelling that might occur due to thermal expansion is not included in the volume changes shown in Fig. 6.

The differences in δ_v between A_0 and R solutions at lower temperatures can be explained by the selective cleavage of oligonucleotide cross-links, discussed previously. However, there is also a smaller difference at higher temperatures where all of the oligonucleotide cross-linkers would be expected to be thermally de-hybridised. It is believed that this is a result of the analyte oligonucleotides hybridising with the thermally cleaved sensor strands, thereby increasing the ionic charge of the macromolecular structure. The increased ionic charge of the macromolecular structure leads to greater swelling. The oligonucleotides of the R solutions will not bind to the macromolecular structure, hence

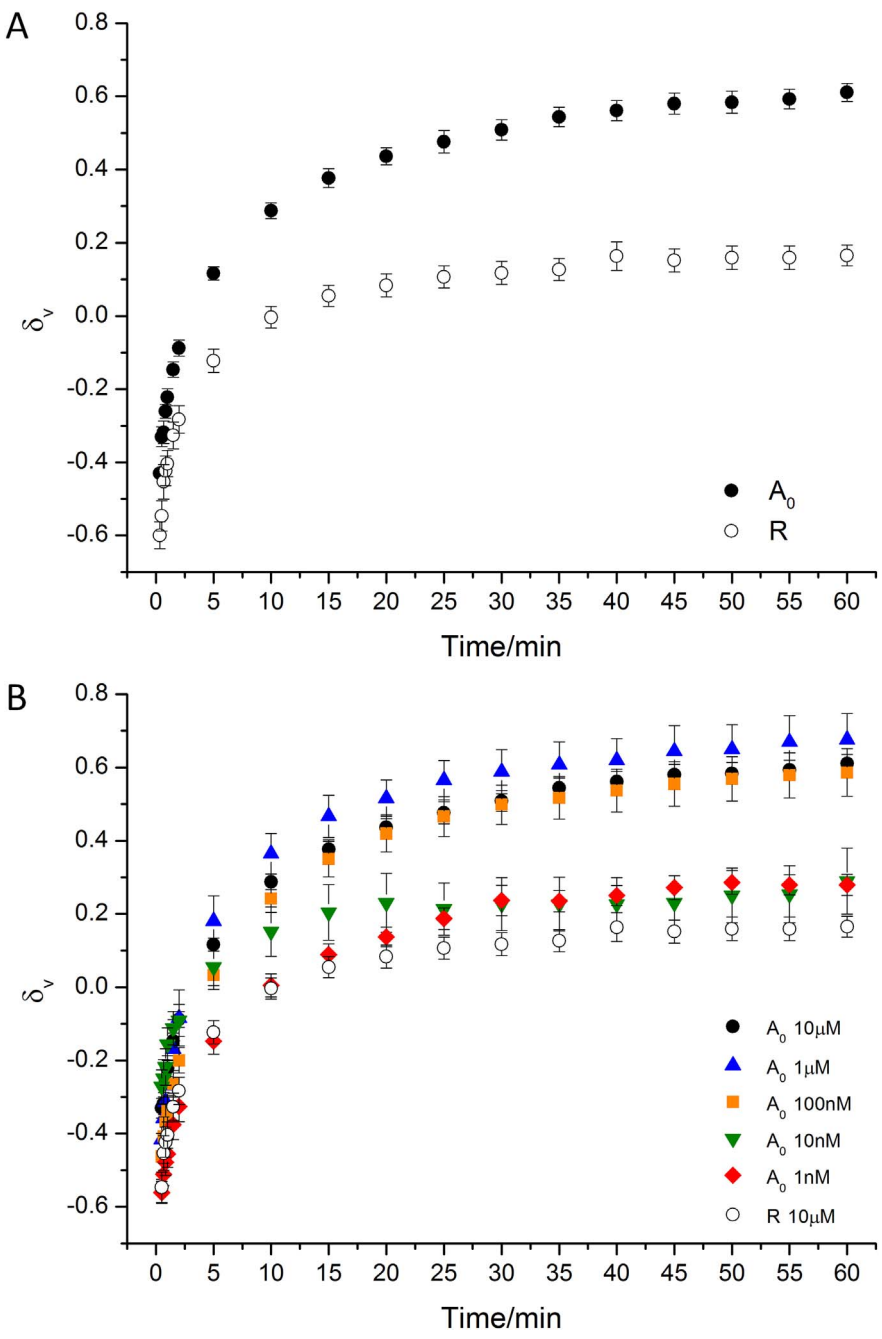

Fig. 4. A: Fractional volume increase with time for oligonucleotide-functionalised composites in A_0 and R solutions of 10 μM, B: Fractional volume increase against time for oligonucleotide-functionalised composites in solutions of varying A_0 concentration and R solution of 10 μM. All solutions were held at 23 °C.

leaving the ionic charge unchanged. Full discussions on how the ionic make-up of hydrogels influence swelling can be found in reviews by Gawel et al. [23] and Richter et al. [24].

Fig. 6 shows that, even for relatively high analyte concentrations, for temperatures up to and including room temperature there is a significant proportion of oligonucleotide cross-linkers that remain uncleaved. Conversely, irrespective of the presence of analyte molecules, a significant proportion of the oligonucleotide cross-linkers will be dehybridised due to thermal effects at approximately 25 °C. This non-specific cross-linker cleavage is undesirable for sensing applications as it constitutes a false-positive response. The variability of δ_v shown in Fig. 6 means that, in their current form, the temperature of OCPCs would need to be controlled below 25 °C if applied to sensing applications.

3.2. Electrical measurements

Fig. 7 shows the direct current (d.c.) electrical resistance of OCPCs swelling in both A_0 and R solutions. In both cases the OCPCs begin in a high conductivity state (of the order 10 kΩ) and transition to a low conductivity state (of approximately 300–400 kΩ), which is a result of the conductive pathways breaking as the polymer swells. There is a clear difference in transition time, with the A_0 solution samples transitioning approximately 40 s before the samples in R solutions. This is indicative of the different rates of swelling that result from the selective cleavage of the oligonucleotide cross-linkers by the analyte molecules, shown using optical measurements in Fig. 4.

A notable difference between Fig. 4 and Fig. 7 is the time at which the plateau is reached. In Fig. 7 the resistance reaches a plateau within 3 min whereas in the optical tests it was observed that an equilibrium

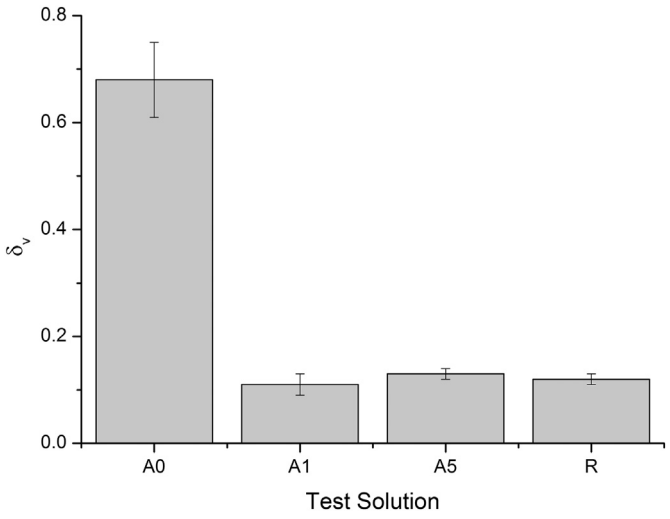

Fig. 5. The fractional volume increase for OCPCs in various oligonucleotide solutions. The solutions contain 1 μM of either a perfectly complementary analyte sequence (A_0), a single-mismatch sequence (A_1), a five-mismatch sequence (A_5) or a random sequence (R). All solutions contain 150 mM NaCl and 1 mM phosphate buffer. All solutions were held at 23 °C.

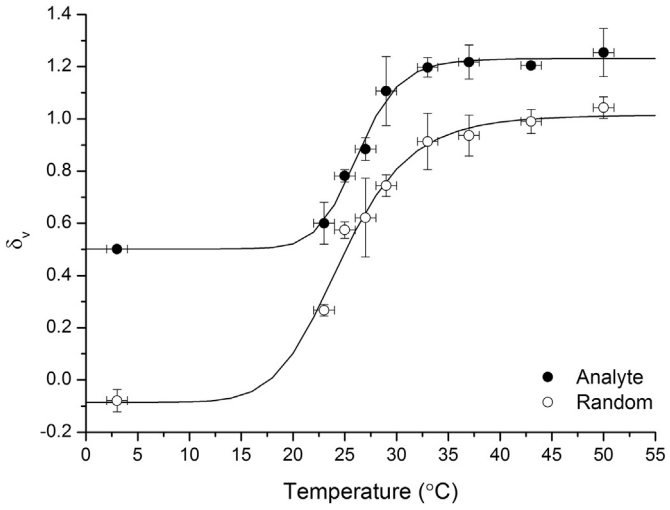

Fig. 6. Fractional volume increase against temperature for OCPCs in 10 μM A_0 and R solutions after 18 h of immersion. Both solutions contain 150 mM NaCl and 1 mM phosphate buffer.

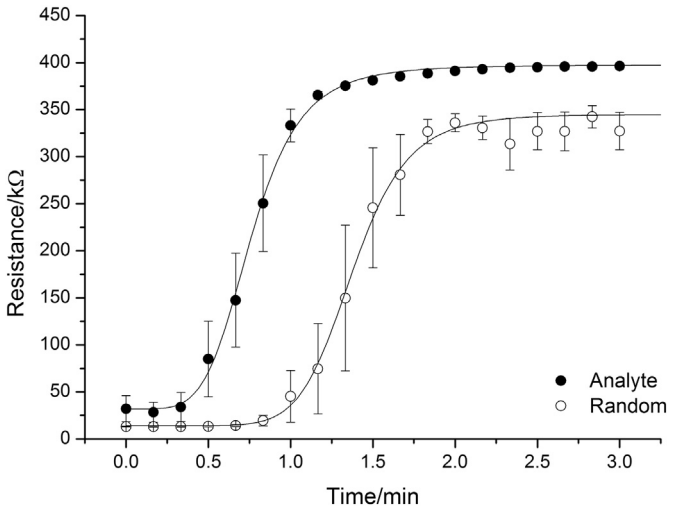

Fig. 7. The d.c. electrical response of OCPCs swelling over time in 10 nM A_0 and R solutions. The solutions were held at 23 °C and contained 150 mM NaCl and 1 mM phosphate buffer.

volume was not reached until times of approximately 1 h. It is clear that the full range of swelling is not being captured in Fig. 7, as the low conductivity state is reached long before the OCPCs reach their maximum volume, and that any swelling after approximately 3 min is not measured electrically. As such, it can be concluded that the difference in final resistance between the A_0 and R samples in Fig. 7 is not the result of the difference in volume that we have already seen. The difference can be explained by considering the difference in conductivity of the oligonucleotide solution. The conductivity of an electrolyte solution depends upon the concentration, charge and mobility of the charge carriers within the solution [25,26]. As per design, in A_0 solutions the analyte oligonucleotides will hybridise with the sensor strands, thereby becoming immobilised within the polymer structure. As such, they will no longer be able to contribute to the conductivity of the solution. In the case of R solutions, the oligonucleotides will remain free in solution and thus contribute to the conductivity. Therefore it is to be expected that OCPCs have lower resistances in solutions containing non-complementary oligonucleotides.

Fig. 8 shows the d.c. electrical resistance or OCPCs swelling in A_0 solutions of varying concentration. For A_0 concentrations above 10 nM there is little difference in the time of transition between the high and low conductivity states (the average value for the midpoint of the curve is (0.73 ± 0.01) minutes) and the rate of change of resistance. At the lower concentration of 1 nM the transition occurs approximately 40 s later, closer to the transition time for OCPCs in R solutions for which the average value of the midpoint of the curve is (1.18 ± 0.09) minutes. This is consistent with what we have seen in Fig. 4 B where for concentrations of 10 nM and above, at early times, there is no discernible difference in volume with differing concentration, whereas for concentrations below 10 nM the swelling response was indistinguishable from that of OCPCs in R solutions.

With the exception of the sample in 10 μM A_0 solution, the resistances for all concentrations tend towards approximately 400 kΩ. The resistance of the 10 μM samples are lower, at approximately 370 kΩ. This is believed to be a result of the solution oligonucleotide concentration being high enough that sufficient numbers of the analyte oligonucleotides remain unbound and contribute to the solution conductivity.

4. Conclusions

We have reported the first steps in an attempt to apply conductive composites, similar to those applied in the field of chemical vapor sensing, to oligonucleotide detection. Such sensors could form the basis of a simple, rapid and low-cost technology for applications ranging from forensic science to disease diagnostics. Analyte solutions can clearly be differentiated from controls, in under 3 min and with single-base specificity, through differences in the rate of resistance change. In their current form the sensors have a relatively high limit of detection of 10 nM, whilst this may be acceptable for some applications, a greater sensitivity would be desirable for many others [27]. However, improvements may be achievable through modifications to the composition (both physical and chemical) of the composites. In addition, printed arrays of small volume OCPC sensors may offer future opportunities for improvements to sensitivity and selectivity through multi-sensor averaging, multiplexing and pattern recognition.

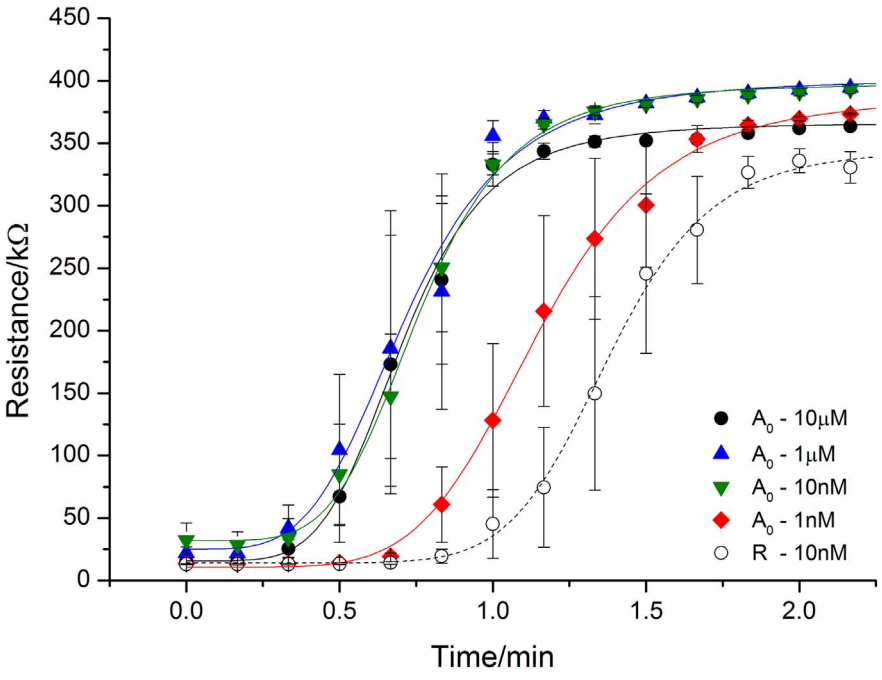

Fig. 8. The d.c. electrical response of carbon nanopowder OCPCs swelling over time in analyte (A_0) solutions of concentrations ranging from 10 μM to 1 nM and a R solution of 10 nM. The solutions were held at 23 °C and contained 150 mM NaCl and 1 mM phosphate buffer.

Conflicts of interest

The work described herein is the subject of patent application WO2017006122 A1.

Acknowledgements

We would like to thank the Engineering and Physical Sciences Research Council (EPSRC) for Impact Acceleration Award Funds EP/K503794/1, and the EPSRC and the School of Engineering at the University of Edinburgh for a PhD studentship for David Ferrier. We would also like to thank Axis-Shield Diagnostics Ltd. for providing materials.

Appendix A. Supplementary data

Supplementary data to this article can be found online at https://doi.org/10.1016/j.sbsr.2017.11.007.

References

[1] M.C. Lonergan, E.J. Severin, B.J. Doleman, S.A. Beaber, R.H. Grubbs, N.S. Lewis, Array-based vapor sensing using chemically sensitive, carbon black-polymer resistors, Chem. Mater. 8 (1996) 2298–2312.
[2] B.J. Doleman, M.C. Lonergan, E.J. Severin, T.P. Vaid, N.S. Lewis, Quantitative study of the resolving power of arrays of carbon black-polymer composites in various vapor-sensing tasks, Anal. Chem. 70 (1998) 4177–4190.
[3] B.J. Doleman, N.S. Lewis, Comparison of odor detection thresholds and odor discriminablities of a conducting polymer composite electronic nose versus mammalian olfaction, Sensors Actuators B Chem. 72 (2001) 41–50.
[4] F. Zee, J.W. Judy, Micromachined polymer-based chemical gas sensor array, Sensors Actuators B Chem. 72 (2001) 120–128.
[5] M.C. Burl, B.C. Sisk, T.P. Vaid, N.S. Lewis, Classification performance of carbon black-polymer composite vapor detector arrays as a function of array size and detector composition, Sensors Actuators B Chem. 87 (2002) 130–149.
[6] Y.S. Kim, S.-C. Ha, Y. Yang, Y.J. Kim, S.M. Cho, H. Yang, Y.T. Kim, Portable electronic nose system based on the carbon black–polymer composite sensor array, Sensors Actuators B Chem. 108 (2005) 285–291.
[7] G. Pioggia, F. Di Francesco, A. Marchetti, M. Ferro, A. Ahluwalia, A composite sensor array impedentiometric electronic tongue part I. Characterization, Biosens. Bioelectron. 22 (2007) 2618–2623.
[8] P. Hands, P. Laughlin, D. Bloor, Metal–polymer composite sensors for volatile organic compounds: part 1. Flow-through chemi-resistors, Sensors Actuators B Chem. 162 (2012) 400–408.
[9] H. Bruck, M. Yang, Y. Kostov, A. Rasooly, Electrical percolation based biosensors, Methods 63 (2013) 282–289.
[10] S. Tierney, B.T. Stokke, Development of an oligonucleotide functionalized hydrogel integrated on a high resolution interferometric readout platform as a label-free macromolecule sensing device, Biomacromolecules 10 (2009) 1619–1626.
[11] M. Gao, K. Gawel, B. Stokke, Toehold of dsDNA exchange affects the hydrogel swelling kinetics of a polymer–dsDNA hybrid hydrogel, Soft Matter 7 (2011) 1741–1746.
[12] K. Gawel, B.T. Stokke, Logic swelling response of DNA–polymer hybrid hydrogel, Soft Matter 7 (2011) 4615–4618.
[13] N. Rosenfeld, et al., MicroRNAs accurately identify cancer tissue origin, Nat. Biotechnol. 46 (2008) 462–469.
[14] N. Kosaka, H. Iguchi, T. Ochiya, Circulating microRNA in body fluid: a new potential biomarker for cancer diagnosis and prognosis, Cancer Sci. 101 (2010) 2087–2092.
[15] W.C.S. Cho, MicroRNAs: potential biomarkers for cancer diagnosis, prognosis and targets for therapy, Int. J. Biochem. Cell Biol. 42 (2010) 1273–1281.
[16] E.K. Hanson, H. Lubenow, J. Ballantyne, Identification of forensically relevant body fluids using a panel of differentially expressed microRNAs, Anal. Biochem. 387 (2009) 303–314.
[17] C. Lux, C. Schyma, B. Madea, C. Courts, Identifcation of gunshots to the head by detection of RNA in backspatter primarily expressed in brain tissue, Forensic Sci. Int. 237 (2014) 62–69.
[18] S. Tierney, D.R. Hjelme, B.T. Stokke, Determination of swelling of responsive gels with nanometer resolution. Fiber-optic based platform for hydrogels as signal transducers, Anal. Chem. 80 (2008) 5086–5093.
[19] T. Tanaka, D.J. Fillmore, Kinetics of swelling of gels, J. Chem. Phys. 70 (1979) 1214–1218.
[20] A. Tichopad, M. Dilger, G. Schwarz, M.W. Pfaffi, Standardized determination of real-time PCR efficiency from a single reaction set-up, Nucleic Acids Res. 31 (2003) e122.
[21] S. Zhao, R. Fernald, Comprehensive algorithm for quantitive real-time polymerasze chain reaction, J. Comput. Biol. 12 (2005) 1047–1064.
[22] A. Spiess, C. Feig, C. Ritz, Highly accurate sigmoidal fitting of real-time PCR data by introducing a parameter for asymmetry, BMC Bioinformatics 9 (2008) 221.
[23] K. Gawel, D. Barriet, M. Sletmoen, B.T. Stokke, Responsive hydrogels for label-free signal transduction within biosensors, Sensors (Basel) 10 (2008) 4381–4409.
[24] A. Richter, G. Paschew, S. Klatt, J. Lienig, K.-F. Arndt, H.-J.P. Adler, Review on hydrogel-based pH sensors and microsensors, Sensors (Basel) 8 (2008) 561–581.
[25] H. Ma, R. Wallbank, R. Chaji, J. Li, Y. Suzuki, C. Jiggins, A. Nathan, An impedance-based integrated biosensor for suspended DNA characterization, Sci. Rep. 3 (2013) 2730.
[26] Y.-S. Liu, P. Banada, S. Bhattacharya, A. Bhunia, R. Bashir, Electrical characterization of DNA molecules in solution using impedance measurements, Appl. Phys. Lett. 92 (2008) 143902.
[27] K. Zen, C.-Y. Zhang, Circulating microRNAs: a novel class of biomarkers to diagnose and monitor human cancers, Med. Res. Rev. 32 (2012) 326–348.